A Dynamic Model for Printed Apertures in Anisotropic Stripline Structures

J. C. da S. Lacava, A. V. Proaño De la Torre, and Lucio Cividanes

***Abstract*—This paper presents a full-wave analysis method for printed apertures in anisotropic stripline structures. Both electric and magnetic anisotropy of the most general form are assumed. Working in the Fourier domain, closed-form expressions for the transformed electromagnetic fields are derived. Special attention is dedicated to the particular case of dielectrics with uniaxial anisotropy. In this case, spectral Green's functions in compact and closed form are obtained. Effects of the anisotropic ratio on the input impedance of a printed slot are presented.**

***Index Terms*—General anisotropy, input impedance, method of moments, printed apertures, spectral domain, stripline structures.**

I. Introduction

THE analysis of the electromagnetic fields created by sources embedded in stratified planar media finds application in many different fields such as optoelectronics, microwave circuitry, and antennas [1]. Often, the planar printed antennas and microwave circuits can exhibit one or more anisotropic layers. These layers can be naturally (e.g., crystalline materials) or artificially anisotropic (as a result of the manner under which they are manufactured or introduced to improve the circuit/antenna performance) [2].

Using a Fourier-transform domain field representation in conjunction with matrix analysis techniques, the radiation from a dipole near a general anisotropic layer has been investigated [3]. Also, the dispersion relation for this general medium has been derived and studied in [4].

Printed aperture in the ground plane of a microstrip line is a versatile radiating element. One particularly interesting application of such a structure is the active antenna phased array, which includes active devices (like phase shifters and amplifiers) in the dielectric layers. The main advantages of this kind of antenna are wider bandwidth, less interaction via surface waves, better isolation and negligible direct radiation from the feed network [5]. This open microstrip structure has been analyzed in the literature [6], and the strong backlobe radiation due to the resonant aperture is its main disadvantage. In order to avoid this undesirable radiation, a stripline can be used to feed the aperture.

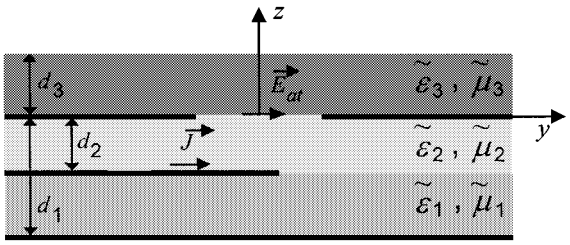

Fig. 1. Geometry of a printed aperture in anisotropic stripline structure.

The purpose of this paper is to present a dynamic model to calculate the electromagnetic fields radiated by apertures in general anisotropic stripline structures. Working in the Fourier domain, expressions for the transformed electromagnetic fields are derived and, consequently, dyadic spectral Green's functions can be determined. This is a very convenient approach to provide efficient application of the method of moments. For brevity, in this paper, only the results obtained for the particular case of three dielectric layers with uniaxial anisotropy are discussed. As the calculation is carried out in the Fourier domain, the spectral Green's functions can be obtained in compact and closed forms. To better visualize the behavior of these functions, a typical three-dimensional (3-D) graphic in the spectral plane is presented. Using the method of moments, the input impedance of a printed slot is calculated. The characteristic equations for the TM and TE modes excited in the uniaxial layers sandwiched between the ground planes are also analyzed.

II. Theory

The structure under consideration consists of a thin conducting strip located at the interface between two anisotropic layers, which are sandwiched between two ground planes. The aperture is printed in the ground plane located on the x–y-plane of a rectangular coordinate system, with a protection layer covering it, as illustrated in Fig. 1. In our formulation, we consider each layer as a linear and homogeneous medium with general anisotropy, i.e., a medium where the electromagnetic properties are described by tensors of permittivity $\tilde{\varepsilon}_n$ and permeability $\tilde{\mu}_n$ (the index $n = 1, 2,$ or 3 identifies each anisotropic layer). The planar interface $z = d_3$ separates the cover layer from the free space region ($z > d_3$, permittivity ε_0, and permeability μ_0).

The theory used in this paper considers the stripline structure as a boundary value problem where the surface electric current density $\vec{J}(x, y)$ on the conducting strip and the tangential electric-field component $\vec{E}_{\rm at}(x, y)$ in the aperture plane are the virtual sources of the electromagnetic fields. Starting from Maxwell's equations, the wave equations in the anisotropic

Manuscript received May 21, 2000; revised November 30, 2000. This work was supported in part by the Conselho Nacional de Desenvolvimento Científico e Tecnológico under Grant 521049/94-6, by the International Civil Aviation Organization under Grant BRA–95/802 (Objective 6), and by the Coordenação de Aperfeiçoamento de Pessoal de Nível Superior.

J. C. da S. Lacava is with the Department of Electronics Engineering, Instituto Tecnológico de Aeronáutica, 12228-900 São Jose dos Campos SP, Brazil.

A. V. Proaño De la Torre was with the Department of Electronics Engineering, Instituto Tecnológico de Aeronáutica, 12228-900 São José dos Campos SP, Brazil. She is now with the Army Polytechnic School, Sangolquí, Ecuador.

L. Cividanes is with the Brazilian Institute for Space Research, 12001-970 São Jose dos Campos SP, Brazil.

Publisher Item Identifier S 0018-9480(02)00746-9.

layers and in the free-space region are determined. In our approach, the wave equations are solved in the Fourier domain and the boundary conditions for the electromagnetic fields are applied at the interfaces $z = 0$, $z = -d_1$, $z = -d_2$, and $z = d_3$. Expressions for the spectral electromagnetic fields are determined by solving the resulting set of equations. Finally, to obtain the fields in the space domain, the inverse Fourier transform is applied.

A. Electromagnetic Fields in General Anisotropic Layers

In this section, the expressions for spectral electromagnetic fields in general anisotropic layers are derived. For time–harmonic variations, assuming time dependence of the form $e^{i\omega t}$, the wave equations for source-free media are given by

$$\nabla \times \left[\tilde{\mu}_n^{-1} \cdot \left(\nabla \times \vec{\mathbf{E}}_n\right)\right] - \omega^2 \tilde{\varepsilon}_n \cdot \vec{\mathbf{E}}_n = 0 \tag{1}$$

$$\nabla \times \left[\tilde{\varepsilon}_n^{-1} \cdot \left(\nabla \times \vec{\mathbf{H}}_n\right)\right] - \omega^2 \tilde{\mu}_n \cdot \vec{\mathbf{H}}_n = 0 \tag{2}$$

with the tensors $\tilde{\varepsilon}_n$ and $\tilde{\mu}_n$, in matrix form, expressed as follows:

$$\tilde{\varepsilon}_n = \begin{bmatrix} \varepsilon_{1n} & \varepsilon_{2n} & \varepsilon_{3n} \\ \varepsilon_{4n} & \varepsilon_{5n} & \varepsilon_{6n} \\ \varepsilon_{7n} & \varepsilon_{8n} & \varepsilon_{9n} \end{bmatrix}$$

and

$$\tilde{\mu}_n = \begin{bmatrix} \mu_{1n} & \mu_{2n} & \mu_{3n} \\ \mu_{4n} & \mu_{5n} & \mu_{6n} \\ \mu_{7n} & \mu_{8n} & \mu_{9n} \end{bmatrix}.$$

Working in the Fourier domain, the following expressions for the transformed field components are obtained. To simplify, we eliminate, in the subsequent equations, the indexes that identify the parameters related to the nth layer, resulting in

$$\mathcal{E}_\eta(k_x, k_y, z) = \sum_{\tau=1}^{4} \mathbf{e}_{\eta\tau} e^{i\gamma_\tau z} \tag{3}$$

$$\mathcal{H}_\eta(k_x, k_y, z) = \sum_{\tau=1}^{4} \mathbf{h}_{\eta\tau} e^{i\gamma_\tau z} \tag{4}$$

where k_x and k_y are the Fourier spectral variables, and $\mathbf{e}_{\eta\tau} = \mathbf{e}_{\eta\tau}(k_x, k_y)$, and $\mathbf{h}_{\eta\tau} = \mathbf{h}_{\eta\tau}(k_x, k_y)$ are functions to be determined ($\eta = x$, y, or z). The propagation constants γ_τ ($\tau = 1, 2, 3,$ or 4) are obtained by solving the fourth-order characteristic equation

$$\gamma^4 - i\Phi_1\gamma^3 - \Phi_2\gamma^2 + i\Phi_3\gamma + \Phi_4 = 0 \tag{5}$$

where

$$\begin{aligned}\Phi_1 = &-i(\mu_9\varepsilon_9)^{-1}\left\{\varepsilon_9\left[k_x(\mu_3+\mu_7)+k_y(\mu_6+\mu_8)\right]\right. \\ &\left.+\mu_9\left[k_x(\varepsilon_3+\varepsilon_7)+k_y(\varepsilon_6+\varepsilon_8)\right]\right\}\end{aligned} \tag{6}$$

$$\begin{aligned}\Phi_2 = &-(\mu_9\varepsilon_9)^{-1}\left\{k_x^2\left[(\varepsilon_3+\varepsilon_7)(\mu_3+\mu_7)+\varepsilon_1\mu_9+\varepsilon_9\mu_1\right]\right. \\ &+k_y^2\left[(\varepsilon_6+\varepsilon_8)(\mu_6+\mu_8)+\varepsilon_5\mu_9\right. \\ &\left.+\varepsilon_9\mu_5\right]+k_xk_y \\ &\times\left[(\varepsilon_3+\varepsilon_7)(\mu_6+\mu_8)+(\varepsilon_6+\varepsilon_8)\right. \\ &\times(\mu_3+\mu_7)+\varepsilon_9(\mu_2+\mu_4) \\ &\left.\left.+\mu_9(\varepsilon_2+\varepsilon_4)\right]+\omega^2\right. \\ &\left.\times\left[-\xi_5\Theta_1-\xi_1\Theta_5+\xi_2\Theta_2+\xi_4\Theta_4\right]\right\}\end{aligned} \tag{7}$$

$$\begin{aligned}\Phi_3 = &(\mu_9\varepsilon_9)^{-1}\left\{k_x^3\left[\varepsilon_1(\mu_3+\mu_7)+\mu_1(\varepsilon_3+\varepsilon_7)\right]\right. \\ &+k_y^3\left[\varepsilon_5(\mu_6+\mu_8)+\mu_5(\varepsilon_6+\varepsilon_8)\right] \\ &+k_x^2k_y\left[\varepsilon_1(\mu_6+\mu_8)+\mu_1(\varepsilon_6+\varepsilon_8)\right. \\ &+(\varepsilon_2+\varepsilon_4)(\mu_3+\mu_7) \\ &\left.+(\varepsilon_3+\varepsilon_7)(\mu_2+\mu_4)\right] \\ &+k_xk_y^2\left[\varepsilon_5(\mu_3+\mu_7)+\mu_5(\varepsilon_3+\varepsilon_7)\right. \\ &+(\varepsilon_2+\varepsilon_4)(\mu_6+\mu_8) \\ &\left.+(\varepsilon_6+\varepsilon_8)(\mu_2+\mu_4)\right] \\ &+\omega^2\left\{k_x\left[\xi_5(\Theta_3+\Theta_7)+\Theta_5(\xi_3+\xi_7)\right.\right. \\ &-\xi_8\Theta_2-\xi_2\Theta_8-\xi_6\Theta_4 \\ &\left.-\xi_4\Theta_6\right]+k_y \\ &\times\left[\xi_1(\Theta_6+\Theta_8)+\Theta_1(\xi_6+\xi_8)\right. \\ &-\xi_3\Theta_2-\xi_2\Theta_3-\xi_7\Theta_4 \\ &\left.\left.-\xi_4\Theta_7\right]\right\}\end{aligned} \tag{8}$$

$$\begin{aligned}\Phi_4 = &(\mu_9\varepsilon_9)^{-1}\left\{k_x^4\varepsilon_1\mu_1+k_y^4\varepsilon_5\mu_5+k_x^3k_y\right. \\ &\times\left[\varepsilon_1(\mu_2+\mu_4)+\mu_1(\varepsilon_2+\varepsilon_4)\right]+k_xk_y^3 \\ &\times\left[\varepsilon_5(\mu_2+\mu_4)+\mu_5(\varepsilon_2+\varepsilon_4)\right]+k_x^2k_y^2 \\ &\times\left[\varepsilon_1\mu_5+\varepsilon_5\mu_1+(\varepsilon_2+\varepsilon_4)(\mu_2+\mu_4)\right] \\ &+\omega^2\left\{k_xk_y\left[\xi_9(\Theta_2+\Theta_4)\right.\right. \\ &+\Theta_9(\xi_2+\xi_4)-\xi_6\Theta_3 \\ &\left.-\xi_3\Theta_6-\xi_8\Theta_7-\xi_7\Theta_8\right] \\ &+k_x^2\left[-\xi_9\Theta_5-\xi_5\Theta_9+\xi_8\Theta_8\right. \\ &\left.+\xi_6\Theta_6\right] \\ &+k_y^2\left[-\xi_9\Theta_1-\xi_1\Theta_9+\xi_3\Theta_3\right. \\ &\left.\left.+\xi_7\Theta_7\right]\right. \\ &\left.+\omega^2\det\left[\tilde{\varepsilon}\right]\det\left[\tilde{\mu}\right]\right\}\end{aligned} \tag{9}$$

$$\det[\tilde{\varepsilon}] = \varepsilon_1\xi_1 + \varepsilon_2\xi_4 + \varepsilon_3\xi_7 \tag{10}$$

$$\det[\tilde{\mu}] = \mu_1\Theta_1 + \mu_2\Theta_4 + \mu_3\Theta_7. \tag{11}$$

The parameters ξ_p and Θ_p ($p = 1, 2, 3, \ldots,$ 8, or 9) are defined as $\Omega_p = \xi_p$ or Θ_p. When $\Omega_p = \xi_p$, then $\varphi_p = \varepsilon_p$ and when $\Omega_p = \Theta_p$, then $\varphi_p = \mu_p$, where

$$\begin{aligned}\Omega_1 &= \varphi_5\varphi_9 - \varphi_6\varphi_8 \\ \Omega_2 &= \varphi_3\varphi_8 - \varphi_2\varphi_9 \\ \Omega_3 &= \varphi_2\varphi_6 - \varphi_3\varphi_5 \\ \Omega_4 &= \varphi_6\varphi_7 - \varphi_4\varphi_9 \\ \Omega_5 &= \varphi_1\varphi_9 - \varphi_3\varphi_7 \\ \Omega_6 &= \varphi_3\varphi_4 - \varphi_1\varphi_6 \\ \Omega_7 &= \varphi_4\varphi_8 - \varphi_5\varphi_7 \\ \Omega_8 &= \varphi_2\varphi_7 - \varphi_1\varphi_8 \\ \Omega_9 &= \varphi_1\varphi_5 - \varphi_2\varphi_4.\end{aligned}$$

The expressions for the electromagnetic fields in the space domain are obtained through the inverse Fourier transform of $\vec{\mathcal{E}}(k_x, k_y, z)$ and $\vec{\mathcal{H}}(k_x, k_y, z)$. For the τth solution of γ and the ηth component of the field, we have

$$\mathcal{E}_{\eta\tau} = \frac{1}{4\pi^2}\int_{-\infty}^{+\infty}\mathbf{e}_{\eta\tau}e^{-i(k_xx+k_yy-\gamma_\tau z)}dk_xdk_y \tag{12}$$

$$\mathcal{H}_{\eta\tau} = \frac{1}{4\pi^2}\int_{-\infty}^{+\infty}\mathbf{h}_{\eta\tau}e^{-i(k_xx+k_yy-\gamma_\tau z)}dk_xdk_y. \tag{13}$$

Introducing (12) and (13) in the Maxwell's curl equations, we can write $\mathbf{e}_{x\tau}$, $\mathbf{e}_{y\tau}$, $\mathbf{h}_{x\tau}$, $\mathbf{h}_{y\tau}$, and $\mathbf{h}_{z\tau}$ as a function of $\mathbf{e}_{z\tau}$ in the following way:

$$\mathbf{e}_{x\tau} = D_\tau^{-1}\left[\alpha_{a\tau} + \alpha_{b\tau} Y_\tau\right]\mathbf{e}_{z\tau} \tag{14}$$

$$\mathbf{e}_{y\tau} = D_\tau^{-1}\left[\alpha_{c\tau} + \alpha_{d\tau} Y_\tau\right]\mathbf{e}_{z\tau} \tag{15}$$

$$\mathbf{h}_{x\tau} = D_\tau^{-1}\left[\alpha_{e\tau} + \alpha_{f\tau} Y_\tau\right]\mathbf{e}_{z\tau} \tag{16}$$

$$\mathbf{h}_{y\tau} = D_\tau^{-1}\left[\alpha_{g\tau} + \alpha_{h\tau} Y_\tau\right]\mathbf{e}_{z\tau} \tag{17}$$

$$\mathbf{h}_{z\tau} = Y_\tau \mathbf{e}_{z\tau} \tag{18}$$

where

$$\alpha_{a\tau} = \{k_x\gamma_\tau(\varepsilon_3 k_x + \varepsilon_6 k_y - \varepsilon_9\gamma_\tau) + \omega^2\left[\gamma_\tau(\mu_7\xi_1 + \mu_8\xi_2) + (\mu_7 k_x + \mu_8 k_y)\xi_3\right]\} \tag{19}$$

$$\alpha_{b\tau} = \left[\omega(\mu_7 k_x + \mu_8 k_y - \mu_9\gamma_\tau)(\varepsilon_8\gamma_\tau - \varepsilon_2 k_x - \varepsilon_5 k_y)\right] \tag{20}$$

$$\alpha_{c\tau} = k_y\gamma_\tau(\varepsilon_3 k_x + \varepsilon_6 k_y - \varepsilon_9\gamma_\tau) + \omega^2\left[\gamma_\tau(\mu_7\xi_4 + \mu_8\xi_5) + (\mu_7 k_x + \mu_8 k_y)\xi_6\right] \tag{21}$$

$$\alpha_{d\tau} = \omega(\mu_7 k_x + \mu_8 k_y - \mu_9\gamma_\tau)(\varepsilon_1 k_x + \varepsilon_4 k_y - \varepsilon_7\gamma_\tau) \tag{22}$$

$$\alpha_{e\tau} = \omega\left[k_x(k_x\xi_6 - k_y\xi_3) + \gamma_\tau(k_x\xi_4 - k_y\xi_1) + \omega^2\mu_8(\varepsilon_1\xi_1 + \varepsilon_2\xi_4 + \varepsilon_3\xi_7)\right] \tag{23}$$

$$\alpha_{f\tau} = k_x\left[k_x(\varepsilon_1 k_x + \varepsilon_2 k_y) + k_y(\varepsilon_4 k_x + \varepsilon_5 k_y) - \gamma_\tau(\varepsilon_7 k_x + \varepsilon_8 k_y)\right] + \omega^2\left[(\mu_8 k_y - \mu_9\gamma_\tau)\xi_7 - k_x(\mu_8\xi_8 + \mu_9\xi_9)\right] \tag{24}$$

$$\alpha_{g\tau} = \omega\left[k_y(k_x\xi_6 - k_y\xi_3) + \gamma_\tau(k_x\xi_5 - k_y\xi_2) - \omega^2\mu_7(\varepsilon_1\xi_1 + \varepsilon_2\xi_4 + \varepsilon_3\xi_7)\right] \tag{25}$$

$$\alpha_{h\tau} = k_y\left[k_x(\varepsilon_1 k_x + \varepsilon_2 k_y) + k_y(\varepsilon_4 k_x + \varepsilon_5 k_y) - \gamma_\tau(\varepsilon_7 k_x + \varepsilon_8 k_y)\right] + \omega^2\left[(\mu_7 k_x - \mu_9\gamma_\tau)\xi_8 - k_y(\mu_7\xi_7 + \mu_9\xi_9)\right] \tag{26}$$

$$D_\tau = \gamma_\tau\left[\gamma_\tau(\varepsilon_7 k_x + \varepsilon_8 k_y) - k_x(\varepsilon_1 k_x + \varepsilon_2 k_y) - k_y(\varepsilon_4 k_x + \varepsilon_5 k_y)\right] + \omega^2\left[(\mu_7 k_x + \mu_8 k_y)\xi_9 + \gamma_\tau(\mu_7\xi_7 + \mu_8\xi_8)\right] \tag{27}$$

$$Y_\tau = \frac{\gamma_\tau\alpha_{c\tau} + k_y D_\tau - \omega(\mu_1\alpha_{e\tau} + \mu_2\alpha_{g\tau})}{\omega(\mu_1\alpha_{f\tau} + \mu_2\alpha_{h\tau} + \mu_3 D_\tau) - \gamma_\tau\alpha_{d\tau}}. \tag{28}$$

With the above procedure, we have drastically reduced the number of unknowns in each anisotropic layer, resulting in only the transformed fields $\mathbf{e}_{z\tau}$ to be determined.

B. Electromagnetic Fields in Free-Space Region

Using a procedure similar to that presented in Section II-A, and suppressing the wave propagating toward negative z since this region is unbounded for $z > d_3$, it is possible to obtain all the fields in the free-space region [7].

C. Boundary Conditions and Spectral Green's Functions

For the stripline structure presented in Fig. 1, after applying the boundary conditions [7], we obtain a set of 14 equations with 14 unknowns. Solving this set of equations, expressions for the transformed electromagnetic fields inside and outside the anisotropic layers are derived. Consequently, dyadic spectral Green's functions can be determined. For brevity, in this paper, only the results obtained for the particular case of three dielectric layers with uniaxial anisotropy are discussed ($\tilde{\mu}_n \to \mu_0$, $\varepsilon_{1n} = \varepsilon_{5n} = \varepsilon_{xn}$, and $\varepsilon_{9n} = \varepsilon_{zn}$). Examples of these functions are as follows:

$$G_{yxM1} = \frac{\varepsilon_{x2}\gamma_{21}k_y^2\sin\left[\gamma_{21}(d_1+z)\right]}{\left(k_x^2+k_y^2\right)\mathrm{TM}_G} + \frac{\gamma_{12}k_x^2\sin\left[\gamma_{11}(d_1+z)\right]}{\left(k_x^2+k_y^2\right)\mathrm{TE}_G} \tag{29}$$

$$R_{xyM2} = \frac{i\omega\varepsilon_{x2}k_xk_y}{\gamma_{22}\left(k_x^2+k_y^2\right)\mathrm{TM}_G} \times \{-\varepsilon_{x2}\gamma_{21}\sin\left[\gamma_{21}(d_1-d_2)\right] \times \sin\left[\gamma_{22}(d_2+z)\right] + \varepsilon_{x1}\gamma_{22}\cos\left[\gamma_{21}(d_1-d_2)\right] \times \cos\left[\gamma_{22}(d_2+z)\right]\} + \frac{i\gamma_{12}k_xk_y}{\omega\mu_o\left(k_x^2+k_y^2\right)\mathrm{TE}_G} \times \{\gamma_{12}\sin\left[\gamma_{11}(d_1-d_2)\right] \times \sin\left[\gamma_{12}(d_2+z)\right] - \gamma_{11}\cos\left[\gamma_{11}(d_1-d_2)\right] \times \cos\left[\gamma_{12}(d_2+z)\right]\} \tag{30}$$

where

$$\gamma_{1n} = \sqrt{\omega^2\mu_o\varepsilon_{xn} - \left(k_x^2+k_y^2\right)} \tag{31}$$

$$\gamma_{2n} = \sqrt{\frac{\varepsilon_{xn}}{\varepsilon_{zn}}\left[\omega^2\mu_o\varepsilon_{zn} - \left(k_x^2+k_y^2\right)\right]} \tag{32}$$

$$\mathrm{TM}_G = \varepsilon_{x1}\gamma_{22}\sin(\gamma_{22}d_2)\cos\left[\gamma_{21}(d_1-d_2)\right] + \varepsilon_{x2}\gamma_{21}\cos(\gamma_{22}d_2)\sin\left[\gamma_{21}(d_1-d_2)\right] \tag{33}$$

$$\mathrm{TE}_G = \gamma_{11}\sin(\gamma_{12}d_2)\cos\left[\gamma_{11}(d_1-d_2)\right] + \gamma_{12}\cos(\gamma_{12}d_2)\sin\left[\gamma_{11}(d_1-d_2)\right]. \tag{34}$$

TM_G and TE_G are the characteristic equations of the TM and TE modes excited in the uniaxial layers sandwiched between the ground planes, G_{yxM1} is the component of the dyadic spectral Green's function in layer 1 that relates $\mathcal{E}_{y1}$ with j_{Mx}, R_{yxM2} is the dyadic component in layer 2 that relates $\mathcal{H}_{x2}$ with j_{My}, $j_{M\upsilon} = j_{M\upsilon}(k_x, k_y)$ is the Fourier transform of the component $J_{M\upsilon}(x,y)$, $\vec{J}_M = \hat{z} \times \vec{E}_a(x,y)$, and $\upsilon = x$ or y.

Since the electromagnetic fields in the space domain are obtained through the inverse Fourier transform, double integrals in the spectral variables k_x and k_y must be calculated. In general, these calculations are numerically complex so that an insightful analysis of the spectral Green's functions must be made. To visualize the typical behavior of these functions, the real part of the complex function G_{yxM1} was computed along the interface $z = -d_2$ and plotted in Fig. 2. The following parameters were used in this computation: $d_1 = 3.0$ mm, $d_2 = 1.5$ mm, $f = 1.0$ GHz, $\varepsilon_{rx1} = 2.1$, $\varepsilon_{rx2} = 2.2$, $\varepsilon_{rz1} = 2.3$, and $\varepsilon_{rz2} = 2.4$ with the same loss tangent $= 0.0018$ for the two uniaxial layers. In this particular configuration, the complex function G_{yxM1} has only one pole. This pole is related to the propagation constant of the fundamental mode that can be excited in the region between the ground planes. The behavior of the real and imaginary parts of G_{yxM1} in the vicinity of the pole is observed in Fig. 3, plotted for $k_x = 0$ and $31.9 < k_y < 32.3$. In this case, the pole is positioned near $k_y = 32.1$rad/m.

Using (33) and (34), dispersion curves for propagating modes in the region between the ground planes, under lossless condition, are plotted in Fig. 4. We can observe from theses curves

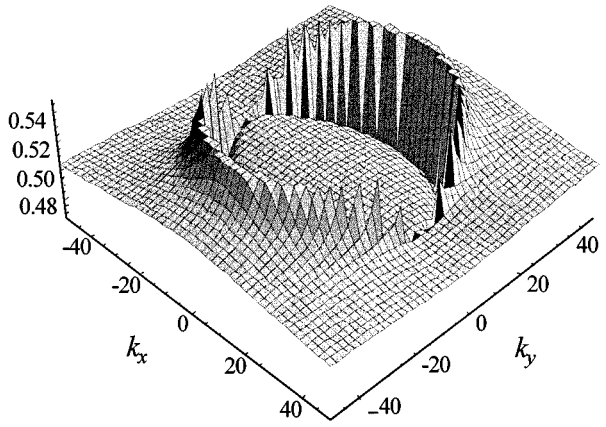

Fig. 2. 3-D graphic for the real part of G_{yxM1}.

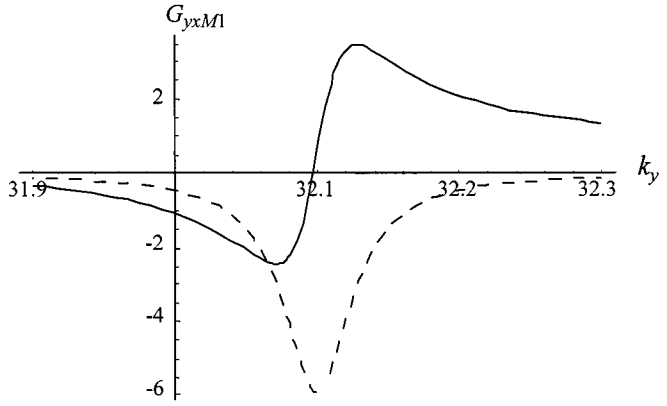

Fig. 3. Behavior of the real and imaginary parts of the complex function G_{yxM1} near the pole position. ——: $\mathrm{Real}[G_{yxM1}]$. – – –: $\mathrm{Im}[G_{yxM1}]$.

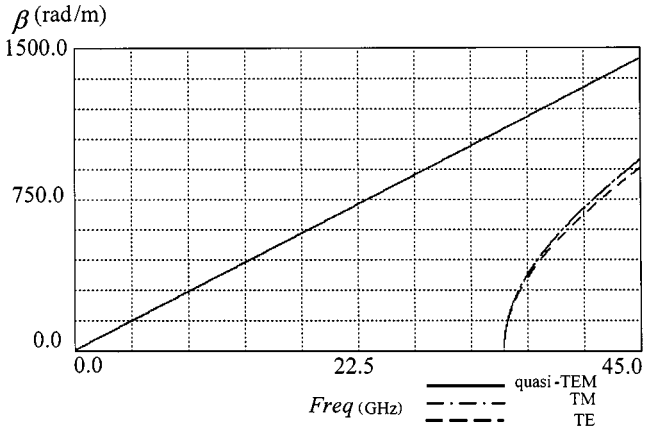

Fig. 4. Dispersion curves for propagating modes in the region between the ground planes.

that: 1) the fundamental mode of propagation is nondispersive (*quasi-TEM* mode) and has no cutoff frequency and 2) for the TM and TE modes, the expected dispersive behavior is obtained.

III. Method of Moments and Input Impedance

Coupled integral equations can be obtained by enforcing the following boundary conditions: the total tangential magnetic field must be continuous across the rectangular slot and the

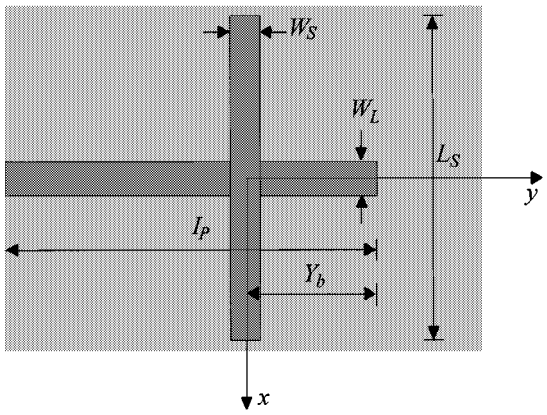

Fig. 5. Plant view of a rectangular slot fed by an open stripline: W_S is the slot width and W_L is the stripline width.

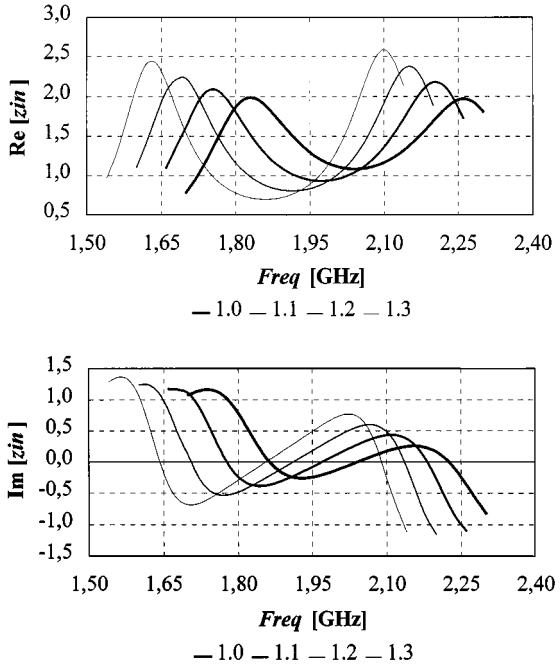

Fig. 6. Graphics for the real and imaginary parts of the normalized input impedance z_{in}.

total tangential electric field must vanish along the stripline surface. These integral equations are solved numerically by the well-known method-of-moments technique. In this approach, the electric current density on the stripline and the tangential electric-field component in the aperture plane are expanded as a set of basis functions. Sinusoids were used to represent incident and reflected traveling waves of the fundamental stripline mode, and triangular subsectional functions were used near the open end. Triangular subsectional functions were also used for the tangential electric-field component in the aperture plane. As test functions, only triangular subsectional modes (with edge conditions) were used. Solving the resulting linear system, tangential electric-field component in the aperture plane, reflection coefficient, and current distribution on the stripline can be obtained. After that, calculating the characteristic impedance (Z_o) and the propagation constant of the stripline, the antenna input impedance can be determined.

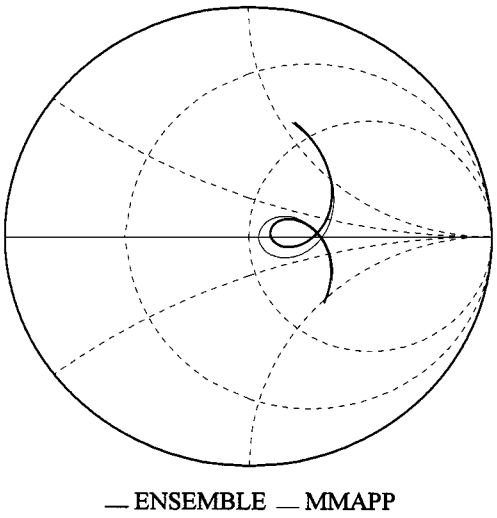

Fig. 7. Normalized input impedance for isotropic case: (1.7–2.3) GHz.

Fig. 5 shows the plant view of a rectangular slot fed by an open-end stripline. For brevity, only results for the antenna with $d_1 = 3.524$ mm, $d_2 = d_3 = 1.524$ mm, $\varepsilon_{rx1} = \varepsilon_{rz1} = 1.0$, $\varepsilon_{rx2} = \varepsilon_{rx3} = 2.55$, loss tangent $= 0.0018$, $L_S = 41.0$ mm, $W_S = 4.0$ mm, $Y_b = 8.8$ mm, $I_p = 110.55$ mm, and $W_L = 5.6$ mm, are presented. Graphics for the normalized input impedance z_{in} ($z_{\text{in}} = Z_{\text{in}}/Z_o$), calculated at $y = -(I_p - Y_b)$, are plotted in Fig. 6 with the following values for the anisotropic ratio $(\varepsilon_{rz}/\varepsilon_{rx})$: 1.0, 1.1, 1.2, and 1.3. As observed, increasing the anisotropic ratio the input impedance is affected by a nonnegligible quantity and the resonant frequency decreases.

For the isotropic case ($\varepsilon_{rz1} = \varepsilon_{rx1} = 1.0$, $\varepsilon_{rz2} = \varepsilon_{rx2} = \varepsilon_{rz3} = \varepsilon_{rx3} = 2.55$), the normalized input impedance calculated from the uniaxial theory is presented in Fig. 7. Good agreement between our calculation (MMAPP) and that obtained by using the software Ensemble[1] is observed.

IV. Conclusions

This paper has described a full-wave technique for analysis of printed apertures in anisotropic stripline structures. This versatile geometry has the advantage of negligible radiation from the feed network, in contrast with the open structure of a printed aperture in the ground plane of a microstrip line. This is an important consideration when designing active phased-arrays antennas in order to avoid the undesirable backlobes.

Working in the Fourier domain, expressions for the transformed electromagnetic fields have been derived. Dyadic spectral Green's functions for the particular case of three dielectric layers with uniaxial anisotropy have been discussed. Typical 3-D graphic in the spectral plane have been presented. Using the method of moments, the input impedance of a printed slot has been calculated. The effect of the anisotropic ratio $(\varepsilon_{rz}/\varepsilon_{rx})$ on the normalized input impedance has been presented. As a result of our calculation, it is clear that by increasing this anisotropic ratio, the antenna input impedance is affected by a nonnegligible quantity, while the resonant frequency decreases. The characteristic equations for the TM and TE modes excited in the uniaxial layers sandwiched between the ground planes have also been analyzed. As expected from similar stripline (isotropic) structures, it has been found that the fundamental mode of propagation is *quasi-TEM* and has no cutoff frequency.

[1]*Ensemble: Design, Review, & 1D Array Synthesis, Version 4.1a*, Boulder Microwave Technologies Inc., Boulder, CO, 1996.

References

[1] F. Mesa, R. Marqués, and M. Horno, "On the computation of the complete spectral Green's dyadic for layered bianisotropic structures," *IEEE Trans. Microwave Theory Tech.*, vol. 46, pp. 1158–1164, Aug. 1998.

[2] N. G. Alexopoulos, "Integrated-circuit structures on anisotropic substrate," *IEEE Trans. Microwave Theory Tech.*, vol. MTT-33, pp. 847–881, Oct. 1985.

[3] J. L. Tsalamengas and N. K. Uzunoglu, "Radiation from a dipole near a general anisotropic layer," *IEEE Trans. Antennas Propagat.*, vol. 38, pp. 9–16, Jan. 1990.

[4] N. J. Damaskos, A. L. Mafett, and P. L. Uslenghi, "Dispersion relation for general anisotropic media," *IEEE Trans. Antennas Propagat.*, vol. AP-30, pp. 991–993, Sept. 1982.

[5] M. Kahrizi, T. P. Sarkar, and Z. A. Maricevic, "Analysis of a wide radiating slot in the ground plane of a microstrip line," *IEEE Trans. Microwave Theory Tech.*, vol. 41, pp. 29–37, Jan. 1993.

[6] F. Croq, "Antennes microrubans multicouches alimentees par ouverture: Appications aux antennes a large bande et haute purete de polarization pour radar et telecommunication spatiale," Ph.D. dissertation, Laboratoire d'Electronique, Univ. Nice-Sophia, Antipolis, France, 1990.

[7] J. C. S. Lacava, A. V. P. De la Torre, and L. Cividanes, "A dynamic model for printed apertures in anisotropic stripline structures," in *Proc. IMOC'99*, Rio de Janeiro, Brazil, CD ROM I124.

J. C. da S. Lacava was born in Caçapava, Brazil, in 1951. He received the B.Sc. degree in electrical engineering from the Faculdade de Engenharia de São José dos Campos, São José dos Campos SP, Brazil, in 1974, and the M.Sc. and the Ph.D. degree in electronic engineering from the Instituto Tecnológico de Aeronáutica (ITA), São José dos Campos, Brazil, in 1979 and 1985, respectively.

In 1976, he joined the staff of the Microwave Group, Department of Electronics Engineering, ITA, and became an Associate Professor in 1985. From 1986 to 1987, he was an Associate Researcher with the Aeronautics and Space Institute (IAE), where he conducted research on cylindrical arrays of microstrip antennas for telemetry systems. His present research interests are in the areas of electromagnetic theory and antennas, with emphasis on microstrip antennas and complex media.

Dr. Lacava is a member of the Brazilian Microwave and Optoelectronics Society (SBMO) and the Brazilian Society of Electromagnetics (SBMAG).

A. V. Proaño De la Torre was born in Quito, Ecuador, in 1971. She received the B.Sc. degree in electronic engineering from the Escuela Politécnica del Ejército (ESPE), Sangolquí, Ecuador, in 1996, and the M.Sc. from the Instituto Tecnológico de Aeronáutica, São José dos Campos SP, Brazil, in 1999.

She was a Project Engineer at the Centro de Investigación Científica y Tecnológica del Ejército, Sangolquí, Ecuador. She is currently with the Army Polytechnic School, Sangolquí, Ecuador. Her current areas of interest include electromagnetic theory, numerical methods, and microstrip antennas.

Lucio Cividanes was born in Rio de Janeiro, Brazil, in 1953. He received the B.Sc. degree in electronic engineering from the Federal University of Rio de Janeiro, Rio de Janeiro, Brazil, in 1975, the M.Sc. degree from the National Institute for Space Research (INPE), São José dos Campos SP, Brazil, in 1978, and the Ph.D. degree from the Instituto Tecnológico de Aeronáutica, São José dos Campos SP, Brazil, in 1992.

His current interests are microstrip antennas and phased arrays for on-board space applications.

Dr. Cividanes is a member of the Brazilian Microwave and Optoelectronics Society (SBMO).